

# Temperature Distribution Study in a Cooled Radial Inflow Turbine Rotor

A. Hamed,\* E. Baskharone,† and W. Tabakoff‡  
University of Cincinnati, Cincinnati, Ohio

In this work, the three dimensional temperature distribution in the cooled rotor of a radial inflow turbine is determined numerically using the finite element method. Some of the results obtained using different cooling techniques with various coolant to primary mass flow ratios are presented for comparison. In this analysis, the complicated geometries of the hot rotor and coolant passage surfaces are handled easily, and the temperatures are determined without loss of accuracy at these convective boundaries. The present work can easily be used in combination with a finite element stress analysis, to investigate the thermal stresses corresponding to the different cooling arrangements.

## Nomenclature

$C_f$	= skin friction coefficient
$D$	= internal cooling passage hydraulic diameter (ft)
$g'''$	= heat generation rate per unit volume (Btu/ft <sup>3</sup> hr)
$[G]$	= heat generation matrix, Eq. (9)
$h$	= convective heat transfer coefficient (Btu/ft hr °F)
$[H]$	= surface convection matrix
$k$	= coefficient of thermal conductivity (Btu/ft hr °F)
$[K]$	= thermal stiffness matrix
$Nu$	= Nusselt number
$\mathbf{n}$	= outward normal unit vector from the rotor surface
$Pr$	= Prandtl number
$\{P\}^t$	= row vector representing the spatial distribution within the element, Eq. (5)
$q$	= heat flux density (Btu/ft <sup>2</sup> hr)
$[R]$	= element nodal spatial matrix, Eq. (6)
$Re$	= Reynolds number
$[SR]$	= thermal boundary load matrix, Eq. (9)
$S_h$	= rotor surface exchanging heat with the hot gas or coolant flow
$S_q$	= rotor surfaces on which heat flux is specified, including adiabatic surfaces
$T$	= temperature (°F)
$V$	= the volume of the tetrahedral element in the finite element representation (ft <sup>3</sup> )
$\{\alpha\}$	= column vector of coefficients, Eq. (5)
$\nu$	= kinematic viscosity (ft <sup>2</sup> /hr)
$\omega$	= rotor angular velocity (radian/hr)
<i>Subscripts</i>	
$x, y, z$	= refer to partial derivation in these directions, respectively
$\infty$	= flow conditions generally in hot gas or coolant flow
<i>Superscripts</i>	
$t$	= transpose of a tensor

## Introduction

In the last decade internal cooling has been used extensively resulting in the continuous increase of turbine inlet

temperatures. Most internal cooling systems are designed using semi-empirical methods to achieve the highest possible effectiveness. Reference 1 presents a review of the present state-of-the-art for the internal cooling of turbine nozzles in aircraft applications.

Experimental studies of air cooled radial inflow turbine rotors are reported in Refs. 2 and 3. Branger<sup>2</sup> investigated the effectiveness of veil cooling on the hub side of the rotor. It was found that the cooling effectiveness was larger at the rotor tip, and decreased as the cooling film is heated and mixed with the hot turbine flow. Petrick and Smith<sup>3</sup> studied the effect of cooling the backside of the rotor on its temperature distribution. While veil and rotor backside cooling techniques are effective for the rotor disk, they induce little variation in the blade temperature. Internal cooling on the other hand can be used to produce the desired reduction in the blade temperature as reported in Ref. 4.

Considering the time and cost associated with experimental studies, computational methods can provide valuable design and development information, concerning the temperature and stress distributions associated with the different turbine cooling techniques. Several studies are available for the temperature distribution in the cooled blades of the axial gas flow turbine blades. They are generally based on two dimensional temperature computations with a spanwise variation in the blade surface convective heat transfer coefficient. In the radial inflow turbine rotor, a similar approach is not possible and the real three dimensional temperature field must be investigated. The finite element method is particularly suitable for handling such complicated geometries without loss of accuracy at the boundaries.

In the present study a numerical method is developed to determine the temperature field in the rotor of a cooled radial inflow turbine. The computations are based on the use of the finite element method, with a variational statement of the three dimensional conduction problem. The various boundary conditions, at the different external and internal cooling surfaces of the rotor are discussed. Different cooling methods and coolant flow rates are investigated and the resulting cooling effectiveness and temperature distributions are reported. The data obtained from the present analysis were found to be in agreement with the available experimental measurements.

## Governing Equations

The field equation for the steady state three dimensional heat conduction problem in an isotropic medium can be expressed as

$$\nabla \cdot (k \nabla T) + g''' = 0 \quad (1)$$

Presented as Paper 76-44, AIAA 14th Aerospace Sciences Meeting, Washington, D.C., Jan. 26-28, 1976; submitted Feb. 11, 1976; revision received June 23, 1976.

\*Associate Professor, Department of Aerospace Engineering, University of Cincinnati, Cincinnati, Ohio. Member AIAA.

†Graduate Research Assistant, Department of Aerospace Engineering, University of Cincinnati, Cincinnati, Ohio.

‡Professor, Department of Aerospace Engineering, University of Cincinnati, Cincinnati, Ohio. Associate Fellow AIAA.

where  $T$  is the temperature,  $k$  the coefficient of thermal conductivity, and  $g''''$  the heat generation rate per unit volume. The boundary conditions associated with the problem under consideration are

$$k \nabla T \cdot \mathbf{n} + h(T - T_\infty) = 0 \text{ on } S_h \quad (2)$$

and

$$k \nabla T \cdot \mathbf{n} + q = 0 \text{ on } S_q \quad (3)$$

In the above equations,  $h$  denotes the convective heat transfer coefficient on the surface  $S_h$ , which convects to the flow at temperature  $T_\infty$ , and  $q$  is the specified heat flux density on the surface  $S_q$ . The union of  $S_h$  and  $S_q$  forms the complete surface boundary  $S$ , whose outward normal unit vector is  $\mathbf{n}$ .

The partial differential Eq. (1) and its boundary conditions (2) and (3) can be cast in the following variational form according to Refs. 5 and 6.

$$I(T) = \frac{1}{2} \int_V [k \left( \frac{\partial T}{\partial x} \right)^2 + k \left( \frac{\partial T}{\partial y} \right)^2 + k \left( \frac{\partial T}{\partial z} \right)^2 - 2g'''' T] dV + \int_{S_h} \left( \frac{1}{2} h T^2 - h T_\infty T \right) dS + \int_{S_q} q T dS \quad (4)$$

where the desired temperature field  $T(x, y, z)$  minimizes the functional " $I$ " over the domain of interest.

### Finite Element Representation

The temperature variation within each element is generally represented by an equation of the form

$$T = \{\mathbf{P}\}' \{\boldsymbol{\alpha}\} \quad (5)$$

where  $\{\mathbf{P}\}'$  is the row vector representing the spatial distribution, and  $\{\boldsymbol{\alpha}\}$  is the column vector of coefficients. The latter can be determined in terms of the values of  $T$  at the nodal points from the following set of simultaneous equations

$$\{T\} = [R]^{-1} \{\boldsymbol{\alpha}\} \quad (6)$$

Equation (5) can therefore be written in terms of the column vector  $\{T\}$  of the nodal temperatures as

$$T = \{\mathbf{P}\}' [R] \{T\} \quad (7)$$

For linear interpolation functions, the integral  $I$  in Eq. (4) can be represented as the sum of the integrals over all the elements. Accordingly we need only to present a single element equation. Substituting the expression given by Eq. (7) into Eq. (4) and performing the variation, leads to the following set of simultaneous equations for the unknown nodal temperatures in the element

$$\begin{aligned} k[R]' \left[ \int_V (\{\mathbf{P}_x\} \{\mathbf{P}_x\}' + \{\mathbf{P}_y\} \{\mathbf{P}_y\}' + \{\mathbf{P}_z\} \{\mathbf{P}_z\}') dV \right] [R] \{T\} \\ + \int_{S_h} h[R]' \{\mathbf{P}\} \{\mathbf{P}\}' [R] \{T\} dS \\ = \int_V [R]' \{\mathbf{P}\} g'''' dV - \int_{S_q} [R]' \{\mathbf{P}\} q dS \\ + \int_{S_h} h[R]' \{\mathbf{P}\} T_\infty dS \end{aligned} \quad (8)$$

More details concerning the derivation of the above equation

may be found in Ref. 7. In this equation the heat generation,  $g''''$ , was chosen to be invariant throughout the element. This approach was adopted since this term was retained in the original formulation to deal with cases involving relatively narrow cooling passages. A heat sink was introduced in such cases to represent the heat absorption by the coolant.

Assembling the equations for all the elements that constitute the rotor body, we obtain a relation of the form

$$[K] \{T\} + [H] \{T\} = [G] - [SR] \quad (9)$$

where  $\{T\}$  is the column matrix of all the rotor nodal temperatures.

Basic linear four node tetrahedrals were chosen in the finite element discretization. The contribution of the conduction, convection, heat generation and heat flux were carried out separately and added to the global matrix. The resulting set of simultaneous algebraic equations given by the last matrix relation were solved using Chelosky's method.<sup>8</sup>

### Calculation of Convective Heat Transfer Coefficients

Empirical formulas are used for the determination of the convective heat transfer coefficients between the rotor and both main and cooling streams. Different cooling configurations are investigated, and the resulting temperature distribution of three of them will be reported later. Besides the one case of external radial outflow of coolant over the rotor backside, two internal cooling configurations were also investigated.

#### Hot Gas Side

The local convective heat transfer coefficient between the blade and the main stream depends on the blade shape, the gas velocity, and the position of the boundary-layer transition point. The highest heat transfer coefficient is found at the blade leading edge, where the laminar boundary layer is thin; its value is determined from the following formula for transverse flow over cylinders.<sup>9</sup>

$$Nu = 1.61 Pr^{0.4} Re^{0.5} \quad (10)$$

where  $Nu$  is the Nusselt number,  $Pr$  is the Prandtl number and  $Re$  is the Reynolds number based on the relative freestream velocity and the blade leading-edge radius.

Turbulent boundary-layer formulation was used in the present study for calculating the convective heat transfer coefficient between the rotor and the hot gas. The following expression for the Nusselt number was used throughout the course of this investigation

$$Nu = \frac{Pr Re (C_f/2)^{0.5}}{(2/C_f)^{0.5} + 5 \{ (Pr - 1) + \phi n [1 + 0.83(Pr - 1)] \}} \quad (11)$$

Where the friction coefficient,  $C_f$ , is evaluated using the following empirical correlation for flat plate

$$C_f = 0.0576 Re^{-0.2} \quad (12)$$

#### Internal Cooling

The flow in the internal cooling passages is affected by the centrifugal and the Coriolis forces. Miyazaki<sup>10</sup> found that the secondary flow is especially suppressed when the cross-sectional aspect ratios are further from unity. Under these conditions, the Nusselt number is very close to that in stationary straight pipes having the same hydraulic diameter. The average Nusselt number for fully developed turbulent flow at high temperatures and heat flux densities is expressed as<sup>11</sup>

$$Nu = \frac{hD}{k} = 0.034 (D/L)^{0.1} Pr^{0.4} Re^{0.8} (T_c/T_s)^{0.8} \quad (13)$$

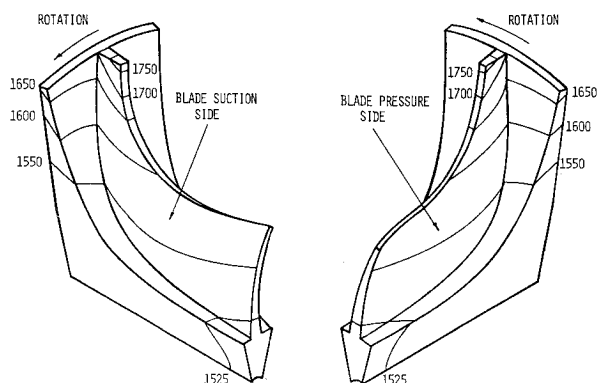


Fig. 1 Rotor temperature distribution without cooling.

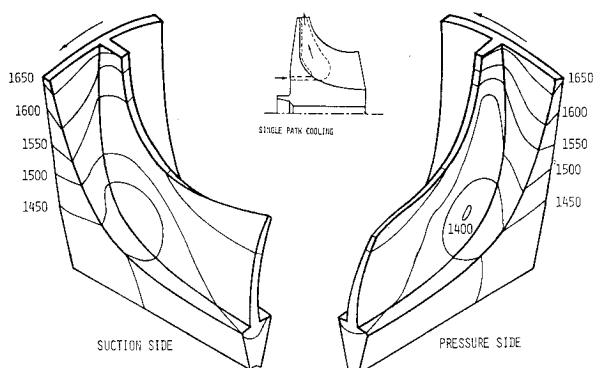


Fig. 2 Rotor temperature distribution with 1.5% internal cooling.

where  $D$  is the hydraulic diameter,  $L$  the passage length,  $T_c$  and  $T_s$  are the coolant and hot passage temperatures, respectively. Both Nusselt and Reynolds numbers are based on the hydraulic diameter, and the flow properties are referenced to  $T_s$ .

#### Rotor Backside Cooling

Petric and Smith<sup>3</sup> experimentally investigated the radial turbine rotor backside cooling by air flowing parallel to the disk in both radially inward and radially outward directions, as well as by air impinging perpendicular to the disk. They found that the radially outward flow resulted in higher values of convection heat transfer coefficients than the radially inward flow. The coolant flow perpendicular to the disk, however, resulted in much higher values of convective heat transfer coefficients compared to those values obtained with flow arrangements parallel to the rotor backside. The experimental data of this reference is so scattered that the authors themselves recommended limiting its application only to the range of the parameters in their study.

Experimentally determined average Nusselt numbers for radially outward flow on a rotating shrouded disk are reported by Haynes and Owen.<sup>12</sup> According to this study, the Nusselt number would approach the free rotating disk values for the high speeds and low coolant flow rates which are involved in radial turbine applications. The free disk correlation was therefore used in the present study to determine the local Nusselt number variation along the rotor backside with the cooling air flowing radially outward. Kreith et al.<sup>13</sup> found that the critical Reynolds number of enclosed rotating disks with source flows is lower than the free disk values. Therefore, neglecting any small laminar core that can exist on the rotor backside, the local Nusselt number at any radius,  $r$ , was calculated using the following equation<sup>14</sup>

$$Nu = \frac{hr}{k} = 0.0195 \left( \frac{\omega r^2}{\nu} \right)^{0.8} \quad (14)$$

where  $\omega$  is the angular velocity of the rotor, and  $\nu$  is the kinematic viscosity.

#### Overall Temperature Computations

The temperature of the cooling stream increases along its flow path due to the heat exchange with the hot rotor. This, in turn, affects the cooled surface temperature as well as the convective heat transfer coefficient. The computations of the rotor and coolant flow temperature distribution must therefore be performed concurrently. The cooling air temperature was evaluated in a separate program in order to achieve the desired accuracy without significantly increasing the storage requirements of the conduction problem. A simple energy balance equation was used to determine the coolant temperature rise.

In carrying out the three-dimensional temperature computations within the rotor, it was assumed that axisymmetric flow conditions prevail at its inlet. The rotor was divided into a number of wedge sectors equal to the number of blades. Each of these sectors included one rotor blade and its corresponding hub section, with the blade at the middle. The heat transfer by conduction between two adjacent rotor sectors as well as the heat transfer by convection at the rotor rim were assumed to be negligible.

#### Results and Discussion

A computer program has been developed to determine the temperature field within the radial inflow turbine rotor. The computations were executed on an IBM 370 time sharing system. The number of nodal points used varied between 300 and 350 per rotor section, depending on the complexity of the coolant passage. The corresponding number of elements were 837 and 1038 for the two internal cooling configurations presented here.

Two previous studies involving external rotor backside cooling<sup>3</sup> and internal blade cooling<sup>4</sup> were available that could be used to verify the results of this study. In Ref. 3 the rotor temperature measurements were reported, but the data supplied in that study was not sufficient to carry out any flow computations, and consequently to determine the convective surface heat transfer coefficients. It was therefore chosen to carry out our computations for a rotor and flow conditions similar to that given in Ref. 4, except for one difference. The rotor disk was extended up to the blade tip to check the ability of our program to handle such complicated three dimensional geometry.

The rotor is made of IN100, a nickel base high temperature alloy, and its tip diameter is 8.2. in. The hot gas inlet total temperature was 2225°F at 67,000 rpm and a turbine flow rate of 4.9 lb/sec. In all the cases investigated, the cooling air total temperature at inlet was assumed to be 850°F. The temperature distributions resulting are presented in the form of plots of isothermal lines on the surface of the blade and its associated hub section.

The computations were first carried out without any cooling flow and the resulting temperature distribution is shown in Fig. 1. Two views, as seen from the blade suction and pressure sides, are represented in the figure. The calculated temperature fields corresponding to two different internal cooling arrangements are presented in Figs. 2 and 3. Figure 2 shows the isothermal lines for 1.5% internal cooling through a single path in the rotor blades, which is later discharged at the rotor tip. It is clear that even for this small amount of coolant mass flow a reduction in the temperatures of 100 to 150°F is achieved in the highly stressed blade regions near the hub.

When the temperature field of Fig. 2 is compared with the computed results of Ref. 4, lower blade temperatures can be observed in the latter data. We must point out, however, that the blade temperatures of Figs. 81 and 82 in that reference were first iterations, which were calculated assuming zero heat flux at the blade hub. According to the same reference, this

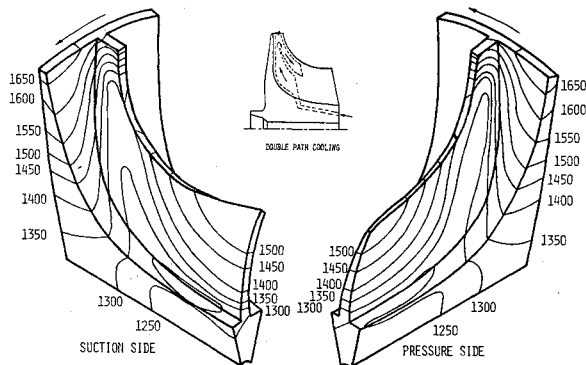


Fig. 3 Rotor temperature distribution with 3% internal cooling.

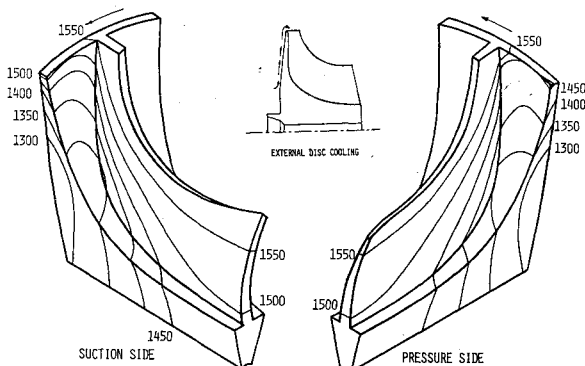


Fig. 4 Rotor temperature distribution with 3% external disk cooling.

can account for about 50°F in lower calculated temperatures at the smaller radius hub sections. The temperature field for 3% internal blade cooling through a double path is shown in Fig. 3. In this arrangement the bulk of the cooling air is discharged on the blade suction side while 1/6 of the coolant is discharged at the tip. The resulting rotor temperature of Fig. 3 were found to be in agreement with those of Ref. 4, in which three iterations were performed to correct for the blade hub heating effects.

Additional results were obtained for 3% rotor disk external radial outflow cooling arrangement and are shown in Fig. 4. It can be observed that the rotor backside temperatures are almost invariant near the axis and up to a radial distance greater than half the tip diameter, then increases sharply towards the tip. The temperature distribution of Fig. 4 can be qualitatively compared with the experimental data given in Ref. 3 for the corresponding cooling arrangement. Although the ratios of coolant to main flow investigated experimentally were generally high in that reference, the temperature measurements at the lowest coolant mass flow of 4% show the same tendencies as our temperature field computations.

In this work we did not intend to present a thermal stress analysis; however, some discussion of the consequences of the temperature fields on the rotor stress distribution can be useful. It is obvious that while internal cooling results in lower blade temperatures, particularly at highly stressed regions near the hub, it also results in relatively high radial temperature gradients as shown in Figs. 2 and 3. This can augment the stresses produced by the centrifugal forces. The rotor external backside cooling might be advantageous in that respect, since it causes mostly axial temperature gradients with the exception of the rotor tip region where the centrifugal loading is insignificant anyway. The stress field produced by centrifugal, thermal and aerodynamic loadings can be deter-

mined using one of the finite element stress analysis programs. Such a task would be greatly facilitated by a finite element heat transfer analysis such as the one presented here. The critical locations of possible creep, rupture or fatigue can be determined. Based on such information, it can be seen whether the external rotor backside cooling with its axial temperature gradient is preferable to the internal cooling, even if double the coolant mass flow is needed to achieve the same metal temperature reduction around the highly stressed blade regions. Keeping in mind the simplicity of manufacturing, this might be the case, even though the losses associated with coolant discharge into the hot stream is another factor to be taken into consideration.

### Conclusions

A useful numerical technique has been developed to predict the three dimensional temperature field in the cooled rotor of a radial inflow turbine. It was found that the finite element method is especially suitable for handling the complicated surface boundaries encountered in the different cooling arrangements. The calculated temperatures obtained using the present method are in good agreement with other analytical methods involving more tedious and time consuming computations. The three dimensional temperature fields, calculated using the present analysis were also found to agree with the available experimental measurements.

### Acknowledgment

This research work was sponsored by NASA Contract No. NAS2-7850, Ames Research Center, Moffet Field, Calif.

### References

- Halls, G.A., "Nozzle Guide Vane Cooling—The State of the Art," AGARD CP-73-71, Paper No. 25.
- Branger, M., "Veil Cooling of Radial Flow Turbines," Final Report prepared by Air Research Manufacturing Co., Ganet Corporation for the Office of Naval Research, Oct. 1963.
- Petrick, E.N. and Smith, R.D., "Experimental Cooling of Radial Flow Turbines," ASME Paper 54-A-245, presented at the Gas Turbine Power Division Annual Meeting, New York, New York, Nov. 28-Dec. 3, 1954.
- Calvert, G.S. and Okapuu, U., "Design and Evaluation of High Temperature Radial Turbine," USAVLABS Technical Report 68-69, Jan. 1969.
- Zienkiewicz, O.C. and Cheung, Y.K., *The Finite Element Method in Structural and Continuum Mechanics*, McGraw Hill, N.Y., 1967.
- Huebner, K.H., *The Finite Element Method for Engineers*, Wiley, N.Y., 1975.
- Baskharone, E., Hamed, A. and Tabakoff, W., "Investigation of Different Cooling Techniques of a Radial Inflow Turbine Rotor Using the Finite Element Method," NASA Report now in preparation.
- Beaufait, W., Rowan, W.H., Hoadley, P.G. and Hackett, R.M., *Computer Methods of Structural Analysis*, Prentice Hall, Englewood Cliffs, N.J., 1970.
- Goldstein, S., *Modern Developments in Fluid Dynamics*, Vol. II, Power Publication, Inc., 1965.
- Miyazaki, H., "Combined Free and Forced Convective Heat Transfer and Fluid Flow in Rotating Curved Rectangular Tubes," *Journal of Heat Transfer*, Feb. 1973, pp. 64-71.
- Humble, L.V., Lowdermilk, W.H., and Desmon, L.G., "Measurements of Average Heat Transfer and Friction Coefficients for Subsonic Flow of Air in Smooth Tubes at High Surface and Fluid Temperatures," NACA Report No. 1020, 1951.
- Haynes, C.M. and Owen, J.M., "Heat Transfer From a Shrouded Disk System With a Radial Outflow of Coolant," ASME Paper 74-GT-4, presented at the Gas Turbine Conference, Zurich, Switzerland, March 31-April 4, 1974.
- Kreith, F., Dougman, E., and Kozlowski, H., "Mass and Heat Transfer From an Enclosed Rotating Disk With and Without Source Flows," *Journal of Heat Transfer*, ASME Series C, Vol. 85, May 1963, pp. 153-163.
- Kreith, F., *Principles of Heat Transfer*, International Textbook Company, 1965.